Acta Cryst. (1998). D**54**, 226–236

Effects of Microheterogeneity in Hen Egg-White Lysozyme Crystallization

B. R. Thomas,* P. G. Vekilov and F. Rosenberger

Center for Microgravity and Materials Research, University of Alabama in Huntsville, Huntsville, Alabama 35899, USA. E-mail: brtprotein@aol.com

(*Received 14 March 1997; accepted 29 July 1997*)

Abstract

In earlier sodium dodecylsulfate–polyacylamide gel electrophoresis (SDS–PAGE) studies it has been found that commonly utilized commercial hen egg-white lysozyme (HEWL) preparations contained 0.2–0.4 mol% covalently bound dimers. Here it is shown, using high-performance capillary electrophoresis (HPCE), that HEWL contains, in addition, two differently charged monomers in comparable amounts. To explore the origin of these microheterogeneous contaminants, purified HEWL (PHEWL) has been oxidized with hydrogen peroxide (0.0026–0.88 *M*) at various pH levels between 4.5 and 12.0. Optical densitometry of oxidized PHEWL (OHEWL) bands in SDS–PAGE gels shows that hydrogen peroxide at 0.88 *M* in acetate buffer pH 4.5 increased the amount of dimers about sixfold over that in commercial HEWL. OHEWL had, in addition to one of the two monomer forms found in HEWL and PHEWL, three other differently charged monomer forms, each of them representing about 25% of the preparation. SDS–PAGE analysis of OHEWL yielded two closely spaced dimer bands with M_r = 28 000 and 27 500. In addition, larger HEWL oligomers with M_r = 1.7 million and 320 000 were detected by gel-filtration fast protein liquid chromatography with multiangle laser light scattering detection. Non-dissociating PAGE in large pore size gels at pH 4.5 confirmed the presence of these large oligomers in HEWL and OHEWL. Increased microheterogeneity resulted in substantial effects on crystal growth and nucleation rate. On addition of 10 μg^{-1} mg ml^{-1} OHEWL to 32 mg ml^{-1} HEWL crystallizing solutions, both the number and size of forming crystals decreased roughly proportionally to the concentration of the added microheterogeneity. The same effect was observed in HEWL solutions on addition of 0.03–0.3 *M* hydrogen peroxide. Repartitioning of the dimer during crystallization at various temperatures between 277 and 293 K was analyzed by SDS–PAGE. The crystals contained $\leq$ 25%(*w*/*w*) of the oligomers in the solution, with no apparent temperature dependence of the repartitioning.

1. Introduction

Recent work has emphasized that impurities or heterogeneities (foreign proteins) can affect the nucleation and growth of protein crystals (for references see Rosenberger *et al.*, 1996; Thomas *et al.*, 1996; Vekilov *et al.*, 1996; McPherson *et al.*, 1996). Most work concentrated on the effects of foreign proteins. However, such effects may also occur in proteins that are highly purified with respect to other proteins, due to the presence of populations of the same protein (microheterogeneities) which differ, for instance, in shape, surface conformation, or charge (Bott *et al.*, 1982; Lorber & Giegé, 1992). Hence, it is likely that to date, most protein crystallization studies, as well as measurements of physical properties of proteins, have utilized heterogeneous and microheterogeneous materials. Because the extent of impurity effects is typically unknown, physical data derived from different protein samples of possibly variable composition are not necessarily applicable to other preparations of the same protein.

During our biochemical characterization of commercial hen egg-white lysozyme (HEWL) we found dimers in concentrations $\geq$ 0.5%(*w*/*w*) or 0.2 mol% in preparations of three major suppliers (Thomas *et al.*, 1996).

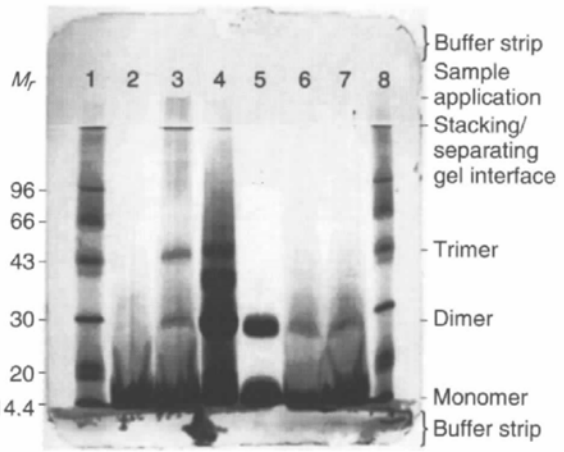

Fig. 1. Treatments of PHEWL to produce dimers. SDS–PAGE 12.5% T Homogeneous Pharmacia PhastGels with silver staining. PHEWL was 10 mg ml^{-1} in CAPS/trisodium phosphate buffer pH 12.0 for each sample with 1 µl loaded in each lane. Lanes: 1, 8 standards; 2, PHEWL control; 3, high ionic strength, 0.5 *M* NaCl; 4, low ionic strength, 10% ethanol; 5, oxidation, 3% H_2O_2 (0.88 M); 6, reducing, 20 m*M* DTT; 7, low oxygen, N_2 sparged.

Hence, these dimers have been present on numerous crystallization experiments in our and other laboratories (Thomas *et al.*, 1996; Vekilov *et al.*, 1995; Vekilov & Rosenberger, 1996; Vekilov *et al.*, 1996; Miyashita *et al.*, 1993, 1994; Ataka, 1995). These dimers withstand the strongly dissociating conditions of the SDS treatment. Furthermore, if they are removed from a sample, they do not reform from a homogeneous monomer population for several weeks (Thomas *et al.*, 1996). Hence, we concluded that these dimers are covalently bound. On removal of the dimers together with higher and lower molecular weight protein impurities, we found that both the growth step velocity on facets of lysozyme single crystals (Vekilov & Rosenberger, 1996) and the crystal quality (Thomas *et al.*, 1996) increased significantly. In this work, we have investigated the origin of the dimer, together with possible effects that it and other microheterogeneities may have on nucleation and crystal growth. Commercial lysozyme is typically prepared under conditions conducive to oxidation. Hence, we have specifically investigated the effects of oxidants on the formation of microheterogeneities.

2. Materials and methods

2.1. *Materials*

We have used lysozyme (Lot No. E 94203) from Seikagaku America (Ijamsville, MD) for all experiments. Buffers, reagents, and trimethylchlorosilane were obtained from Sigma (St Louis, MO). A Milli-RO/Milli-Q water purification system by Millipore (Bedford, MA) was used to provide 18 MΩ water.

2.2. *Fast protein liquid chromatography (FPLC)*

The FPLC system used was a basic Pharmacia Biotech (Piscataway, NJ) gradient instrument with a 280 nm fixed wavelength detector, two pumps and a controller/integrator. Gel-filtration FPLC (GF-FPLC) was performed with a Pharmacia Biotech HiLoad 26/60 Superdex 200 High Performance preparative scale column and a Pharmacia Biotech Superose 12 HR 10/30 analytical scale column. The columns were calibrated for relative molecular weight separations with standard proteins in a kit, MW-GF-70, and the high molecular weight proteins, horse spleen ferritin (M_r = 440 000) and bovine thyroglobulin [$M_r \simeq$ 670 000 monomer (a homodimer of $M_r \simeq$ 330 000 subunits) and 1 300 000 dimeric oligomer], all from Sigma. For calibrations, $M_r >$ 1 000 000 protein standards are scarce. Hence, a Wyatt Technologies (Santa Barbara, CA) miniDAWN multi-angle laser light scattering detector (MALLS) was used in combination with the UV detector in the FPLC system to directly determine protein molecular weights, utilizing the Wyatt Astra software (Wyatt, 1993).

2.3. *Treatments to determine dimer origin*

HEWL was purified (PHEWL) by cation-exchange FPLC as described in Thomas *et al.* (1996). The 280 nm absorbance of solutions was measured and converted to HEWL concentration with 2.64 AU = 1 mg ml^{-1}. Various hydrogen peroxide (H_2O_2) concentrations were obtained by diluting a commercially supplied 30% solution = 8.8 *M* (Everse *et al.*, 1994). To create dimers and higher oligomers, PHEWL solutions, with 10 mg ml^{-1} protein in 20 m*M* CAPS/sodium phosphate–NaOH buffer at pH 12.0, were either oxidized with 3% hydrogen peroxide (0.88 *M*) in buffer, or reduced with 10 m*M* dithiothreitol (DTT, Cleland's Reagent) in buffer. High ionic strength [*I*] samples contained 0.5 *M* NaCl in buffer, while low [*I*] samples contained 10%(*v*/*v*) ethanol in buffer. To lower their O_2 concentration, one set of solutions was sparged with N_2. All samples were held at 278 K for one week, then analyzed by SDS–PAGE.

2.4. *Dimer formation dependence on hydrogen peroxide concentration*

Hydrogen peroxide concentration effects on dimer formation were investigated by adding between 0.0026 and 0.88 *M* H_2O_2 to PHEWL samples containing 10 mg ml^{-1} protein in 20 m*M* CAPS/sodium phosphate–NaOH buffer at pH 12.0. After 16 h at 278 K the solutions were analyzed by SDS–PAGE.

2.5. *Polyacrylamide gel electroporesis*

Analyses were carried out with a PhastGel system electrophoresis unit (Pharmacia). SDS separations were performed with 12.5% Homogeneous and 8–25% gradient PhastGels. For native PAGE analyses we used 4–15% gradient PhastGels (1–2% C) at pH 4.5 with reversed electrodes. An enhanced silver staining protocol adapted for use with the PhastGel system (Heukeshoven & Dernick, 1985) was employed. The gels were scanned for optical densitometric quantification (Patton, 1995).

2.6. *Capillary electrophoresis*

High-performance capillary electrophoresis (HPCE) (Jorgenson & Lukacs, 1983) was utilized to determine charge differences in HEWL and OHEWL. Note that this technique can resolve single charge differences, as demonstrated with acetylated insulin by Whitesides group (Gao *et al.*, 1995). We used a SpectraPHORESIS 100 instrument (Thermo Separations Products, San Jose, CA) with a 75 μm inner diameter, 362 μm outer diameter, 70 cm length, 50 cm detection length, bare fused silica capillary (Polymicro Technologies, Inc., Phoenix, AZ). HEWL samples were separated in 4 m*M* trisodium phosphate capillary buffer pH 12.0 at 15 kV applied voltage (20 μA) with 1 s hydrodynamic (vacuum) injection and 280 nm detection. The high pH was

chosen to exceed the isoelectric point (pI = 11.4) of HEWL. This induced a negative charge on the HEWL molecule, which was necessary for good resolution of the differently charged protein species and eliminated HEWL binding to the capillary wall. Separations below the pI, *e.g.* at pH 4.5 with triethylamine–acetate buffer gave poor resolution.

2.7. *Crystallization*

Batch crystallization incubations (100 µl volume) were performed in 96-well (microwell) plates, which were sealed with transparent tape, and then held at 293 ± 1 K. The samples contained 0.1 *M* sodium acetate buffer pH 4.5, 4%(*w*/*v*) sodium chloride and HEWL at 32 or 16 mg HEWL ml^{-1}. Photographs were made with Polaroid 55 Professional Positive/Negative 4X5 Instant Sheet Film in a WILD Photoautomat MPS 45 controlled Polaroid camera mounted on a WILD Photomakroskop M400 (WILD, Heerbrugg, Switzerland) at a magnification of 12.5 or 32. These photographs were the basis of the quantitative analysis for oxidation effects on crystallization. A 2 cm^2 area of the photographs was used to count the number of crystals and to measure the longest dimension of each crystal. Each photograph was representative of nine replicate wells. These data were normalized with those obtained in nine control wells of the same plate.

2.8. *Induction of microheterogeneity*

OHEWL to be added to crystallizing solutions was made by oxidizing 10 mg ml^{-1} HEWL with 0.88 *M* hydrogen peroxide for 16 h at 278 K in 0.1 *M* sodium acetate buffer pH 4.5. This OHEWL was added into 32 mg ml^{-1} HEWL crystallizing samples in concentrations of 100 µg ml^{-1} to 10 mg ml^{-1} (0.31–31%). Titrations of hydrogen peroxide effects on crystallization were carried out by adding hydrogen peroxide diluted in crystallizing buffer to yield 0.03–0.3 *M* in the 16 (mg HEWL) ml^{-1} crystallizing samples.

2.9. *Repartitioning of heterogeneities in HEWL crystals*

The solution for the repartitioning studies contained 50 mg ml^{-1} HEWL. It was prepared by dissolving the protein in 50 m*M* sodium acetate buffer with pH 4.5. A calculated volume of 10%(*w*/*v*) of NaCl solution in the same buffer was added to bring the precipitant concentration to 2.5%(*w*/*v*). After filtering through a 0.22 µm pore size filter to remove large solid particles, the HEWL concentration was determined by UV spectrophotometry. Then the solution was divided into nine samples of 0.5 ml that were sealed into tubes. Pairs of tubes were kept for 15 d at 277, 283, 288 and 293 K, respectively. For analysis, the crystals were separated from the mother liquor (supernatant) by decanting into an empty tube. To remove the solution layer adhering to the crystal surface, the crystals were twice rinsed with 273 K water. Then the crystals were dissolved in 0.5 ml acetate buffer. Aliquots were taken from the 17 tubes (containing initial solution, supernatants and dissolved crystals) and their concentration was adjusted to 10 mg ml^{-1} by dilution or ultrafiltration. Then the protein compositions of these samples were analyzed using SDS–PAGE, and quantified by scanning densitometry. Note that each gel lane was loaded with the same solution volume (0.3 µl) such that band intensities are representative of the relative concentrations of impurity per lysozyme. To assure quantitative comparability, the gels were run and stained simultaneously.

3. Results and interpretation

3.1. *Size and charge heterogeneity in native and oxidized HEWL*

3.1.1. *Induction of microheterogeneity.* To possibly determine the source of the dimer found in the commercial lysozyme preparations, we subjected PHEWL to a series of treatments. The resulting microheterogeneity was analyzed by SDS–PAGE (Fig. 1). As shown by lane 2, the PHEWL control does not contain dimers. Lane 3 shows that high pH and ionic strength [I] induced covalent dimer formation. On the other hand, low [I] with added organic solvent resulted in a precipitate. On solubilization with SDS, this precipitate yielded various oligomers in large amounts (lane 4) that did not form with other treatments. Oxidation with 0.88 *M* hydrogen peroxide induced the formation of a distinct covalent dimer band (lane 5). At the pH 12 used for Fig. 1, the amount of dimers was 1%(*w*/*w*) or 0.6 mol% determined by quantitative scanning densitometry of dimer bands in SDS–PAGE. This is twice the concentration found in as-received HEWL (Thomas *et al.*, 1996). In another experiment (not shown), we found that at pH 4.5 in sodium acetate buffer, the same hydrogen peroxide treatment resulted in 3.3%(*w*/*w*) or 2 mol% dimers, *i.e.*, about six times the concentration typically present in HEWL.

Sophianopoulos & Van Holde (1964), using equilibrium sedimentation in ultracentrifugation, were the first to observe HEWL (muramidase) dimers that formed at high pH. In contrast to their dimers, however, only a fraction of our dimers dissolved when brought to low pH by the addition of acetic acid, probably due to degradation of the dimers. Hence, we conclude that the dimers observed in our work are not those observed by these authors. However, dimers and other oligomers, that were more recently observed in cross-linking studies (Wang *et al.*, 1996), closely resemble the SDS–PAGE results in our Fig. 1, lane 4, induced by ethanol.

Under reducing conditions (lane 6) with 20 m*M* DTT treatment, some dimers were formed. but, in contrast to high [I] samples, no covalently bound oligomers larger than the dimer were apparent. With low oxygen

conditions, *i.e.*, in samples sparged with nitrogen, again only dimers were formed. Thus, in contrast to hydrogen peroxide oxidation, which was effective at any pH, dimer formation under reducing or low oxygen conditions required high pH.

PHEWL, with no treatment to reduce oxidation, did not form dimers for at least one month after purification when held at 278 K and high concentration (100 mg ml^{-1}) in closed tubes. The SDS–PAGE technique has a treatment protocol designed to completely dissociate proteins which includes high temperature (373 K), strong reducing conditions (2 m*M* DTT) and high detergent concentration [2%(*w*/*w*)]. The fact that this technique did not dissociate the dimer is an effective indicator of a strong covalent attachment rather than a tenuous association. This eliminates any possibility of the dimer as a product of an equilibrium association.

Most commercial HEWL is partially purified by high-pH crystallization in the presence of high salt concentrations. The above findings show that this combination favors dimer formation by oxidation. Hence, we conclude that the dimers present in commercial preparations are likely to be the result of oxidation that cannot be reduced by DTT.

3.1.2. *Dependence of dimer formation on hydrogen peroxide concentration.* The dependence of dimer generation on H_2O_2 concentration was investigated by titrating PHEWL solutions with decreasing concentrations of hydrogen peroxide (0.88–0.0026 *M*) at pH 12. Fig. 2 presents a subset of these analyses in the range of 8 to 2.6 m*M* (in caption: 3 m*M*) hydrogen peroxide. A concentration dependence is apparent, with 2.6 m*M* H_2O_2 producing approximately 15% of the dimers that formed at 8 m*M*. Thus, rather low H_2O_2 concentrations

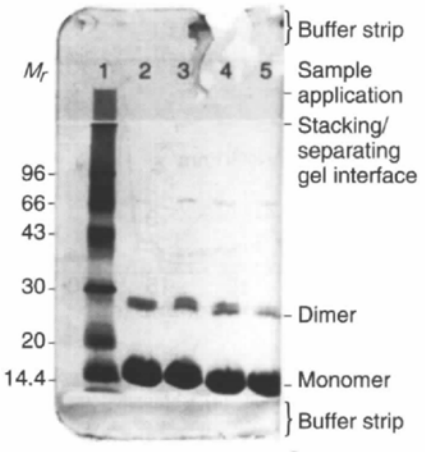

Fig. 2. Titration of PHEWL oxidation with H_2O_2 to produce dimers. SDS–PAGE 12.5% T Pharmacia PhastGels with silver staining. PHEWL was 10 mg ml^{-1} in CAPS/trisodium phosphate buffer pH 12.0 for each sample with 1 µl loaded in each lane. Lanes: 1, standards; 2, PHEWL + 8 m*M* H_2O_2; 3, + 5 m*M* H_2O_2; 4, + 4 m*M* H_2O_2; 5, + 3 m*M* H_2O_2.

suffice to generate detectable dimers. At pH 4.5, similar results were obtained. These results suggested that HEWL contained one or more easily oxidized amino-acid residues.

Surprisingly, Fig. 2 shows two bands for the dimers (molecular weights 28 000 and 27 500) which were masked by the greater band density in other analyses with higher hydrogen peroxide concentrations. This explains the greater width and diffuse nature of the hydrogen peroxide dimers band (Fig. 1) compared to that obtained with commercial HEWL. We speculate that the two dimer forms differ by either the amino-acid residues involved in the attachment between two monomers, or one or two amino-acid residues as a result of amino or carboxyl terminal cleavage. The SDS detergent masked charge differences, therefore only molecular weight differences were observed. Because the dimers in commercial HEWL have only one molecular weight in SDS–PAGE analysis, it appears that the hydrogen peroxide oxidation generated an additional dimer species with necessarily different and physical properties.

3.1.3. *Charge microheterogeneity.* Fig. 3 presents the capillary electrophoresis results obtained with HEWL and OHEWL. The two major peaks and the underlying minor peak in Fig. 3(*a*) indicate that about 50%(*w*/*w*) of the as-received HEWL possesses microheterogeneity in the form of charge differences. HEWL dissolved in the pH 12 buffer yielded identical HPCE results after 10 min or one week in solution. Thus, the buffer has either an instantaneous or no effect on HEWL charge. Although our earlier ion-exchange separations suggested some charge differences (Thomas *et al.*, 1996), such a large amount of microheterogeneity in the bulk enzyme was unexpected. In similar experiments, another commercial HEWL preparation (Sigma) and PHEWL gave nearly identical results. This suggests that such pronounced charge microheterogeneity may be common in HEWL samples.

As shown in Fig. 3(*b*), in OHEWL samples the charge microheterogeneity was increased to about 75%(*w*/*w*). The corresponding three new major peaks had migration times (mt) of 7.25, 8.05 and 8.40 min, *i.e.* shorter than the 8.22 and 8.80 min of the original two major peaks. The shorter mt suggests that the new OHEWL forms have greater positive charge, *i.e.*, a higher p*I* than the starting protein. This indicates that the primary effect of oxidation is the conversion of amino-acid residues to a less acidic and/or more basic form. Furthermore, one can conclude that deamidation (amide hydrolysis) of Asn or Gln to their respective acids, Asp and Glu, does not occur at pH 12 during the period examined, otherwise a more negative charge would result. It also appears that the 8.80 min peak in the control sample was partially converted to the faster migrating peak at 8.4 min in the oxidized sample and the 8.22 min control peak to the faster migrating 7.25 and 8.05 min peaks. Approximately 75% of the total protein was oxidized to three more

positively charged monomers, but only a small proportion formed dimers. Of the two large original peaks in HEWL only a portion of the 8.8 min mt peak remained after oxidation. Thus, OHEWL contained oligomers and monomers with different mass and charge than HEWL.

3.1.4. *Size microheterogeneity.* Fig. 4(*a*) shows a chromatogram with UV and MALLS detection for a GF separation of HEWL. The molecular weights for peaks 1 and 2 are 1.7 million and 320 000, respectively. The large size of the oligomer accounts for the strong light scattering peak 1, that was obtained despite the low underlying protein concentration. Fig. 4(*b*) shows these peaks on a more sensitive scale. The many MALLS peaks at lower molecular weight in Fig. 4(*a*) possibly correspond to the covalently bound oligomers observed in the SDS–PAGE analysis of the HEWL purification performed at pH 11 (Thomas *et al.*, 1996).

The GF-FPLC-MALLS results from a 1 mg OHEWL load presented in Fig. 4(*c*) indicates that, in addition, high molecular weight oligomers with M_r = 1–2 $\times 10^6$ were formed by oxidation. Deconvolutions of peaks 1 in Figs. 4(*a*) and 4(*b*), and peaks 1 and 2 in Fig. 4(*c*) (Wyatt, 1993) indicated considerable polydispersity. The concentration of these oligomers is 2 μg (mg OHEWL)$^{-1}$ or 0.2%(*w*/*w*), *i.e.* one order of magnitude higher than in the as-received lysozyme. Peak 3 Fig. 4(*c*) is dimer, peak 4 is monomer and peak 5 is unknown although it is not composed of peptides as determined by SDS–PAGE.

The HEWL oligomers were also analyzed by native PAGE. Due to the small charge difference of the lysozyme species (see Fig. 3) differentiation in this mode is predominantly by native molecular weight. Since the aggregates in this native gel were not treated with dissociating or reducing agents, and were separated in a pH 4.5 sodium acetate buffered solution, the results can

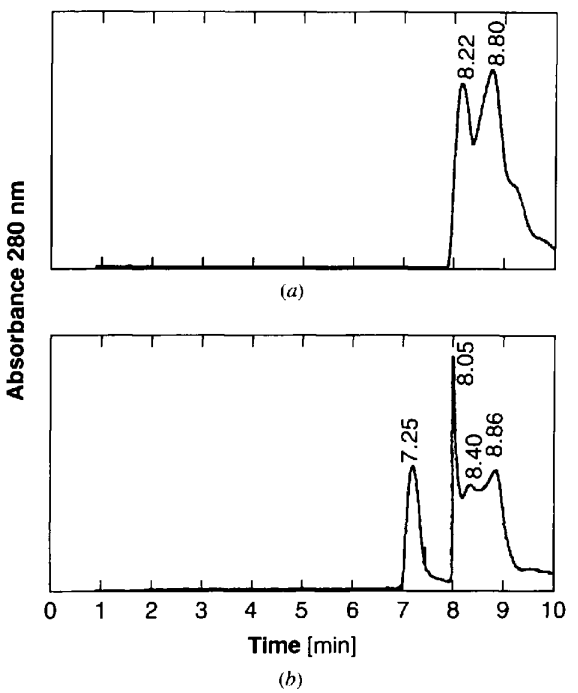

Fig. 3. Capillary electrophoresis separation of differently charged HEWL with oxidatively induced microheterogeneity. (*a*) HEWL in 40 m*M* trisodium phosphate buffer pH 12.0. (*b*) OHEWL in 40 m*M* trisodium phosphate buffer pH 12.0 treated for 16 h with 0.88 *M* H_2O_2 at 278 K. A SpectraPHORESIS 100 instrument with a 75 μm ID, 362 μm OD, 70 cm L, 50 cm detection length bare fused silica capillary was used to separate HEWL samples in 4 m*M* trisodium phosphate buffer pH 12.0 at 15 kV applied voltage (20 μA) with a 1 s hydrodynamic (vacuum) injection and 280 nm detection.

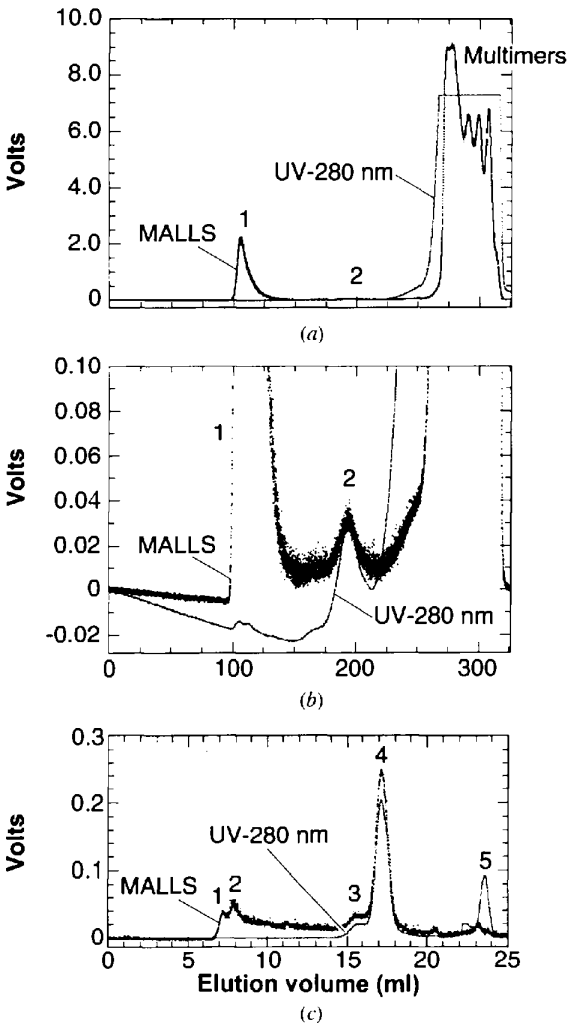

Fig. 4. Characterization of HEWL oligomers with gel-filtration FPLC and light-scattering detection. (*a*) Chromatogram at full scale, (*b*) bottom part of same chromatogram at expanded scale. A HiLoad Superdex 200 gel-filtration column (2.6 cm ID, 60 cm L) was used in a Pharmacia FPLC system with simultaneous miniDAWN light scattering and 280 nm detection. The 1 g HEWL sample at pH 12.0 was separated in 50 m*M* Tris–HCl pH 8.3 containing 200 m*M* NaCl at a flow rate of 1 ml min^{-1}. (*c*) chromatogram of a 1 mg OHEWL separation on an analytical scale Superose 12 GF-FPLC column with MALLS detection. For peak assignments see text.

be expected to be representative of crystallizing solutions. While lane 1 in Fig. 5 was a control sample of HEWL without oxidation treatment, lane 2 was the same HEWL oxidized with 0.88 *M* hydrogen peroxide. A diffuse dimer band is observed above the monomer band, with low resolution due to the large pore size gel used. At the interface between the stacking and separating gels layers we see high molecular weight oligomers ($M_r \geq 1 \times 10^6$). These oligomers were probably the same as those found in the GF-FPLC-MALLS analysis of OHEWL (Fig. 4*c*). The pH 12 HEWL control in lane 3 contained oligomers similar to those observed in the GF-FPLC-MALLS results (Fig. 4*a*). The high molecular weight oligomers above the stacking gel/separating gel interface in lane 4 containing OHEWL oxidized at pH 12 likely correspond to the $M_r = 1.7$ million peak in the GF-FPLC-MALLS separation. The monomer bands in Fig. 5 and the monomer peak in Fig. 4(*c*) (peak 4) correspond to the peaks observed in Fig. 3. Minor components such as dimer or high *Mw* aggregates were not directly observed in the charge analysis with HPCE which was directed at bulk microheterogeneity determinations.

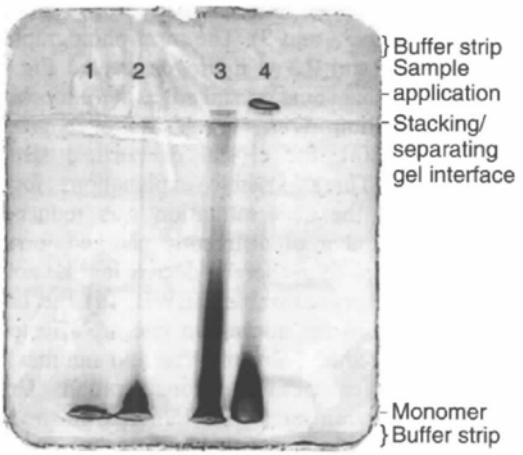

Fig. 5. Characterization of high molecular weight HEWL oligomers utilizing non-dissociating PAGE at pH 4.5 in a large pore size gel. Native PAGE Pharmacia 4-15 Gradient PhastGels with silver staining. PHEWL was 10 mg ml^{-1} for each sample and 1 µl loaded in each lane. Lanes: 1, HEWL in 20 m*M* sodium acetate pH 4.5 control; 2, HEWL in 20 m*M* sodium acetate pH + 0.88 *M* H_2O_2; 3, HEWL in 20 m*M* trisodium phosphate pH 12.0 control; 4, HEWL in 20 m*M* trisodium phosphate pH 12.0 + 0.88 *M* H_2O_2.

3.2. *Microheterogeneity effects and repartitioning during crystallization*

3.2.1. *Effects of oxidation-induced microheterogeneity on crystallization*. Fig. 6 summarizes the effects of added microheterogeneity on nucleation and crystal growth. Three major features can be distinguished. First, in samples with 0.3 mg [0.9%(*w*/*w*)] or less OHEWL added, a small number (~10 crystals ml^{-1}) of relatively larger crystals (0.8 mm length) formed after 24 h and before 48 h. In samples with 0.4–0.5 mg [1.2–1.5%(*w*/*w*)] OHEWL, this required 168 h. No large crystals appeared within 336 h in samples containing 1 mg OHEWL. While the size of these larger crystals was diminished by increasing OHEWL addition, the number of crystals was only slightly reduced.

Second, after 48 h and clearly occurring as a separate event, many crystals on average five times smaller (0.16 mm length) formed within 168 h in all samples except those with 1 mg OHEWL added. Increasing

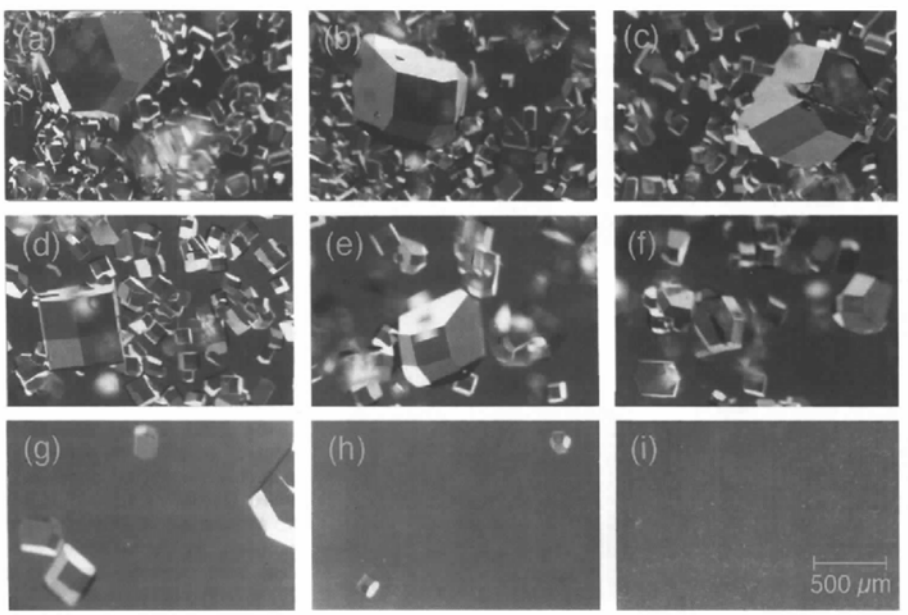

Fig. 6. OHEWL effects on HEWL crystal formulation. OHEWL at the following concentrations was added to a 32 mg ml^{-1} HEWL crystallization solution in microwell plates: (*a*) control – no OHEWL added, (*b*) 0.03%(*w*/*w*) (0.01 mg), (*c*) 0.15%(*w*/*w*) (0.05 mg), (*d*) 0.3%(*w*/*w*) (0.1 mg), (*e*) 0.6%(*w*/*w*) (0.2 mg), (*f*) 0.9%(*w*/*w*) (0.3 mg), (*g*) 1.2%(*w*/*w*) (0.4 mg), (*h*) 1.5%(*w*/*w*) (0.5 mg) and (*i*) 3%(*w*/*w*) (1.0 mg) (≃1 µm particles). The crystallizing solutions were incubated for one week at 293 K before photography.

amounts of added OHEWL resulted in fewer of these smaller crystals, but the average crystal size remained the same up to 0.5 mg OHEWL (Fig. 6).

Third, in samples containing 0.4, 0.5 and 1 mg [1.25, 1.56, 3.13%(*w*/*w*)] OHEWL small particles approximately 1 μm in diameter formed within 168 h. The samples containing 1 mg OHEWL developed only these particles. While the large and small crystals also formed in control samples, the one-micron particles appeared only in samples with OHEWL added. Similar particles have been observed in other HEWL crystallizations and may have been the result of oxidation (Giegé & Ducruix, 1992).

The decrease of both the crystal growth rate (decrease in large crystal size) and nucleation rate (decreasing number of small crystals) with increasing OHEWL concentration, are quantitatively presented in Fig. 7. It should be emphasized that the control samples also contained two crystal sizes. Since the HPCE data also reveal charge microheterogeneity of the HEWL, we speculate that the two different crystal sizes were caused by independent crystallization of microhomogeneous HEWL populations that differed in charge.

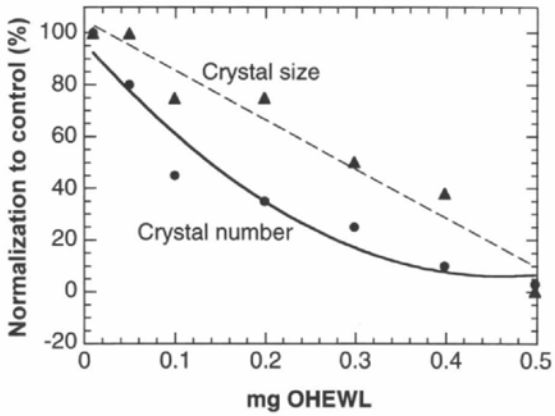

Fig. 7. Quantitative analysis of OHEWL effects on crystallization derived from Fig. 6 photographs. Controls were 20 crystals 2 cm^{-2} for crystal number and 0.8 mm width for crystal size.

The effects of oxidative microheterogeneity was also studied by directly adding 0.03–0.88 *M* hydrogen peroxide to 16 mg ml^{-1} HEWL crystallization solutions. Compared with controls, crystal number and size decreased linearly with increasing hydrogen peroxide concentration (Figs. 8 and 9). The inset photographs for control Fig. 8(*a*) and 0.3 *M* hydrogen treated Fig. 8(*d*) samples indicate that some crystal edges were rounded as a result of oxidation. With 0.88 *M* hydrogen peroxide treatment, Fig. 8(*e*), the crystal or particle size approached 1 μm. Three possible explanations for this behavior are: (i) the supersaturation was reduced by increasing the number of differently charged forms of HEWL from two to four, thereby decreasing the amount of homogeneous, crystallizable HEWL; (ii) the crystal growth rate and (iii) the nucleation rate are affected, as reflected by the reduced crystal size and number with increasing hydrogen peroxide concentration. Crystal growth and nucleation rates were inhibited in the same concentration-dependent manner (Fig. 9) as with OHEWL additions (Fig. 7). Oxidatively induced microheterogeneity in the concentration range of that present in untreated HEWL (HPCE results) created significant changes in the crystallization behavior. Thus, we see that microheterogeneities at concentrations typically considered unimportant in crystallization experiments can significantly affect crystal growth and nucleation rates.

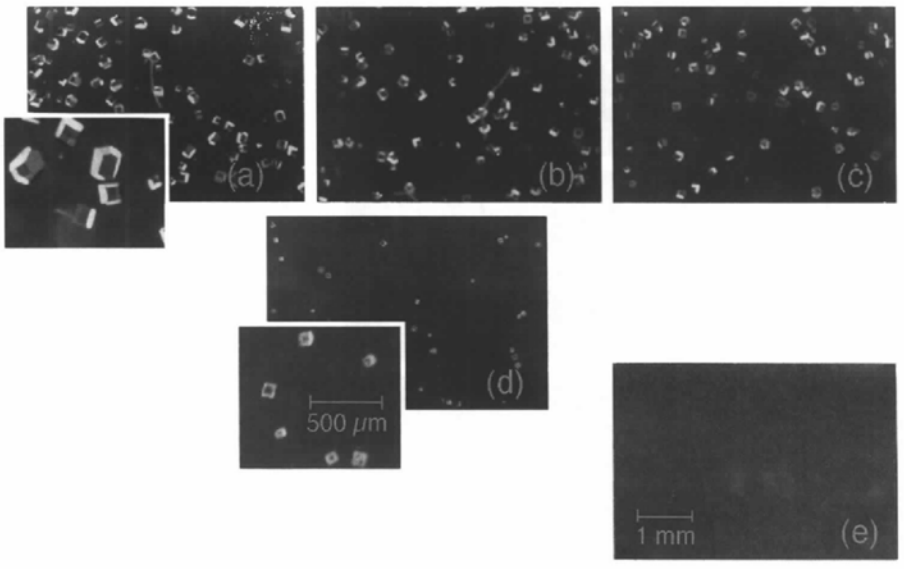

Fig. 8. Oxidation effects on HEWL crystal formation. Hydrogen peroxide at the following concentrations was added to a 16 mg HEWL ml^{-1} crystallization solution in microwell plates: (*a*) control – no hydrogen peroxide added, (*b*) 0.03 *M*, (*c*) 0.09 *M*, (*d*) 0.3 *M* and (*e*) 0.88 *M* (~1 μm particles). The crystallizing solutions were incubated for 48 h at 293 K before photography.

3.2.2. *Repartitioning of impurities between HEWL crystals and mother liquor.* All crystallization runs conducted at 277, 283, 288 and 293 K yielded crystals. The control sample, which was held at 298–300 K, yielded no crystals. In the other samples, between tens (293 K) and thousands (277 K) of crystals were present at the end of the crystallization time. The size of the crystals was uniform (under different crystallization conditions than those described above) at each temperature, but varied from approximately 100 μm at 277 K to 500 μm at 293 K.

Fig. 10 presents the SDS–PAGE analyses of the crystallization runs. Scanning densitometry results for some of these lanes are given in Fig. 11. One sees that the dimer with $M_r \simeq 28\,000$ and an $M_r \simeq 18\,000$ impurity were partially incorporated into the crystal at all temperatures; no significant temperature dependence of the incorporated concentrations is apparent. At all temperatures used, the dimer-to-monomer ratio in the crystals is at least four times lower than in the respective supernatant; *i.e.* the covalently bound dimer is predominantly rejected by the growing interface. This implies that the structural and/or chemical characteristics of these dimers are such that the repulsion between monomer and dimers is stronger than between two monomer molecules. Hence, these dimers cannot be an essential building block for the crystallization of HEWL and the reasons for the slow growth of protein crystals should be sought in other features of the process. This is further supported by our independent finding that in the absence of dimers, HEWL crystal growth is substantially faster (Vekilov & Rosenberger, 1996).

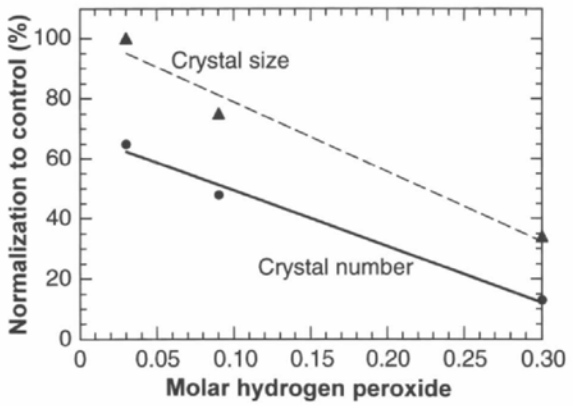

Fig. 9. Quantitative analysis of oxidation effects on crystallization derived from Fig. 8 photographs. Controls were 23 crystals 2 cm^{-2} and 0.28 mm width.

4. Discussion

We have seen that microheterogeneity can decrease the rate of both nucleation and crystal growth of HEWL. Microheterogeneity resulting from charge differences in proteins, *e.g.* human alpha fetoprotein (Keel *et al.*, 1990) and size differences, *e.g.* cholesterol esterase dimeric and monomeric isoforms (Kaiser *et al.*, 1994), are common among proteins *in vivo* and *in vitro.* For cholesterol esterases, these differences have also been shown to have significant effects on crystallization.

These microheterogeneity effects are similar to those obtained by other authors on contamination of a protein preparation with foreign proteins (heterogeneity). For instance, HEWL nucleation and crystal growth rates decreased on addition of turkey egg-white lysozyme and other avian lysozymes (Abergel *et al.*, 1991). Similar

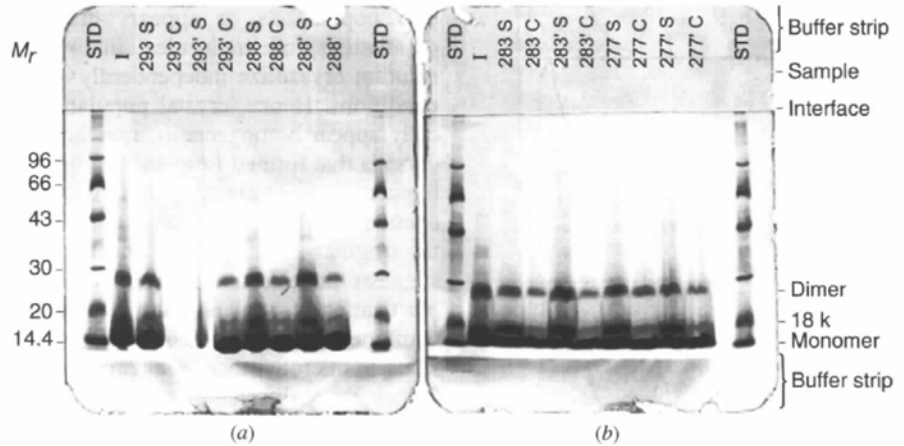

Fig. 10. Analysis of impurity partitioning in HEWL crystals by electrophoresis. SDS–PAGE 12.5% T Homogeneous Pharmacia PhastGels with silver staining. HEWL was concentrated or diluted to 10 mg ml^{-1} for each sample with 0.3 μl loaded in each lane. Lanes 1 and 12: standards (std); lane 2: initial (I) solution control. Lanes are labeled by crystallization temperature, *e.g.* 293 = 293 K sample denoted by S and C are from supernatant and crystal, respectively. Primes denote replicates. The lanes labeled 293 C and 293 ′S were lost as a result of evaporation of those samples (0.3 μl) on the sample applicator. Gels were run and stained simultaneously.

effects were also obtained in studies by Giegé and coworkers (Giegé *et al.*, 1986; Lorber & Giegé, 1992; Lorber *et al.*, 1993; Skouri *et al.*, 1995).

With respect to the induction of microheterogeneity in HEWL, we have seen that hydrogen peroxide, a mild oxidant, is very effective. This is not surprising, since mild oxidation of proteins has been shown to cause large effects. For instance, in lens crystallin proteins, *in situ* production of hydrogen peroxide caused oxidative degradation that lead to cataract formation (Hunt *et al.*, 1992).

In some portions of this study, HEWL was handled at a high pH which might increase the rate of deamidation of Asn and Gln to Asp and Glu amino-acid residues. However, no change in the HEWL was observed over a period of two weeks under these conditions. Other studies have shown that deamidation occurred over a period of several days to years (Liu, 1992). Thus, our observed microheterogeneity at high pH was not the result of high pH buffering.

In a previous study of impurity repartitioning during HEWL crystallization at 277 K, from a solution containing 18 mg ml^{-1} protein and otherwise identical to those used here, dimer incorporation in the crystals was not detected (Vekilov *et al.*, 1996; Rosenberger *et al.*, 1996). However, since the mass concentration of the dimers in the dry materials is ~1% (Thomas *et al.*, 1996), the solution contained 0.18 mg ml^{-1} dimers, as compared with 0.5 mg ml^{-1} in the present experiments. The comparison of these two results indicated that the segregation of the dimers upon crystallization is a strong function of its mother liquor concentration. This is similar to the repartitioning behavior found in numerous inorganic systems (Rosenberger, 1979).

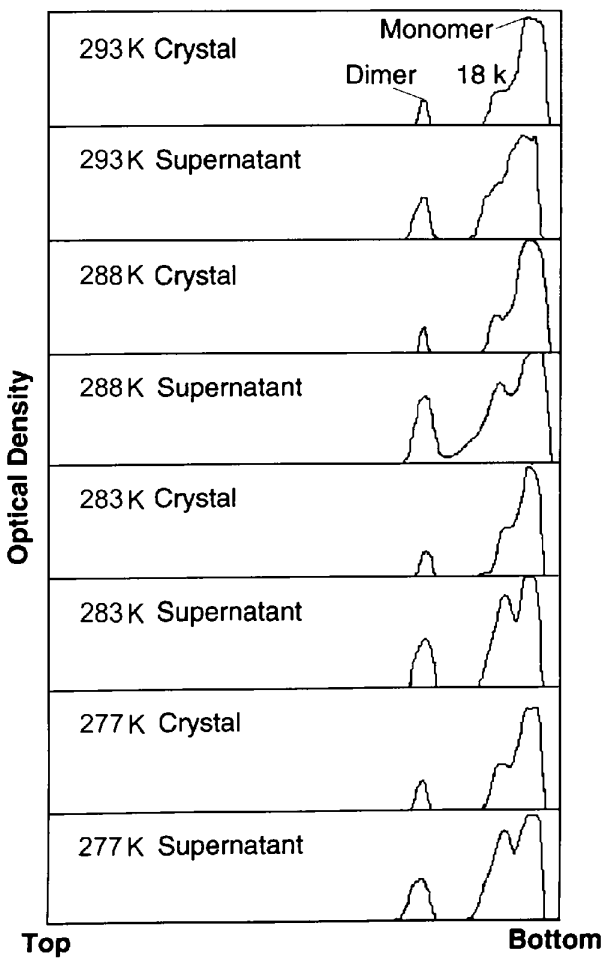

Fig. 11. Optical density scans of some lanes in Fig. 10.

It has been suggested to us on various occasions that the above microheterogeneities are the result of association between the self-interacting protein molecules, as has been described, for instance, by Wills *et al.* (1980). This interpretation is tempting since under the above crystallization conditions there is, indeed, a weak attraction between the lysozyme particles in the solution (Muschol & Rosenberger, 1995, 1996; Ducruix *et al.*, 1996). Note, however, that 'self-association' concepts view oligomer formation as the result of equilibria in an initially homogeneous population of particles, while the oligomers found here are the result of irreversible reactions (oxidation). This, as mentioned before is manifested by (i) the high strength of the bonds that withstand even the strongly dissociating conditions of the SDS treatment, and (i) by the fact these oligomers can be removed, without being reformed from the homogeneous monomer population for several weeks. Hence, the above oligomers must be understood as contaminants rather than an intrinsic result of self-interaction.

Beyond the above reduction in nucleation and growth rates by the microheterogeneous contaminants, this study brings to light another possible complexity in crystallization from even well purified and characterized protein samples. As suggested by the distinctly different crystal size populations, it appears that microhomogeneous populations of molecules in a microheterogeneous solution crystallize independently at somewhat different conditions. Hence, crystal populations that macroscopically appear homogeneous, may actually be mixtures of crystals that formed from each of the microhomogeneous populations. These populations will be much less contaminated by molecules of other populations than the original solution. This and the above repartitioning suggests an effective (though tedious) means of ultra purification of small amounts. Repeated re-crystallization combined with selection of crystal size populations could result in microhomogeneous protein crystals that result in higher X-ray diffraction resolution.

Microheterogeneity may also affect crystal polymorphisms. Specifically, with HEWL, the formation at high temperature (Jollès & Berthou, 1972; Ataka & Tanaka, 1986) or high pH (Steinrauf, 1959) of the orthorhombic crystal form may be influenced by microheterogeneities. Similarly one could speculate that the effects of different

inorganic ions, such as nitrate, nitrite and thiocyanate, on the formation of monoclinic and triclinic crystal forms (Harata, 1994; Riès-Kautt & Ducruix, 1996) can also depend on the specific microheterogeneity of a preparation. Currently, these possibilities are difficult to quantify even with modern biochemical and chromatographic techniques.

While some of the above considerations are speculative, the fact remains that HEWL, the protein most widely used for fundamental crystal growth studies, possesses even in the purest preparations microheterogeneity populations of the order of 50%(*w*/*w*). Since this has not been taken into account in the past, various physical effects attributed to other factors may actually be the result of variations in microheterogeneity between HEWL samples. This is likely to limit the quantitative reproducibility of crystal growth and properties studies, unless diligent attention is paid to the presence and characterization of microheterogeneity.

Unfortunately, microheterogeneity analyses are inhibited by the lack of highly resolving techniques. Of the techniques utilized in this work only HPCE can provide resolution of microheterogeneity that results from small or single charge differences (Jorgenson & Lukacs, 1983; Gao *et al.*, 1995). HPCE is a purely analytical methodology with little utility for preparative separations. With proteins other than HEWL, isoelectric focusing can provide resolution adequate for both analytical and small preparative separations for proteins populations that differ by charge (Bott *et al.*, 1982). GF-FPLC-MALLS provides adequate resolution for analytical and bulk preparative separations of populations that substantially differ by conformation or size, but the theoretical and empirical resolution possible is orders of magnitude less than that of HPCE or isoelectric focusing. Ion-exchange FPLC or high-performance liquid chromatography (HPLC) can provide some preparative capability for charge separations, but often relatively large charge differences ($\gg$HPCE) are required for good resolution. Reversed-phase HPLC (RP-HPLC) is a high-resolution technique suitable for the analysis of microheterogeneity that resolves proteins based on their denatured hydrophobic moieties (Sairam, 1991). The problem with this technique and the reason it was not used here is that in many cases the denaturation is irreversible. Thus, analysis of the effects of charge microheterogeneity in crystallization are limited by methods which provide little protein for experimentation, while analysis of the effects of molecular size microheterogeneity are limited by low resolving power relative to HPCE.

M. Muschol contributed significantly through numerous stimulating discussions. M. Chen at Wyatt Technologies Corp. kindly advised us on some interpretations of the light-scattering data. L. Carter competently prepared the graphs. Research support was provided by the National Aeronautics and Space Administration under Grants NAG8-1161 and NAG8-1168.

References

Abergel, C., Nesa, M. P. & Fonticella-Camps, J. C. (1991). *J. Cryst. Growth*, **110**, 11–19.
Ataka, M. (1995). *Prog. Cryst. Growth Charact.* **30**, 109–128.
Ataka, M. & Tanaka, S. (1986). *Biopolymers*, **25**, 337–350.
Bott, R. R., Navia, M. A. & Smith, J. L. (1982). *J. Biol. Chem.* **257**, 9883–9886.
Ducruix, A., Guilloteau, J. P., Riès-Kautt, M. & Tardieu, A. (1996). *J. Cryst. Growth*, **168**, 28–39.
Everse, J., Johnson, M. C. & Marini, M. A. (1994). *Methods in Enzymology*, edited by J. Everse, K. D. Vandegriff & R. M. Winslow, Vol. 231, p. 549. San Diego: Academic Press.
Gao, J., Mrksich, M., Gomez, F. A. & Whitesides, G. M. (1995). *Analyt. Chem.* **67**, 3093–3100.
Giegé, R., Dock, A. C., Kern, D., Lorber, B., Thierry, J. C. & Moras, D. (1986). *J. Cryst. Growth*, **76**, 554–561.
Giegé, R. & Ducruix, A. (1992). *Crystallization of Nucleic Acids and Proteins. A Practical Approach*, edited by A. Ducruix & R. Giegé, p. 3. Oxford: IRL Press.
Harata, K. (1994). *Acta Cryst.* D**50**, 250–257.
Heukeshoven, J. & Dernick, R. (1985). *Electrophoresis*, **6**, 103–112.
Hunt, J. V., Jiang, Z. Y. & Wolff, S. P. (1992). *Free Radic. Biol. Med.* **13**, 319–323.
Jollès, P. & Berthou, J. (1972). *FEBS Lett.* **23**, 21–23.
Jorgenson, J. W. & Lukacs, K. D. (1983). *Science*, **222**, 266–272.
Kaiser, R., Erman, M., Duax, W. L., Ghosh, D. & Jornvall, H. (1994). *FEBS Lett.* **337**, 123–127.
Keel, B. A., Harms, R. L., Leal, J. A. & Cho, S. (1990). *Mol. Reprod. Dev.* **27**, 281–287.
Liu, D. T. (1992). *Trends Biotechnol.* **10**, 364–369.
Lorber, B. & Giegé, R. (1992). *Crystallization of Nucleic Acids and Proteins. A Practical Approach*, edited by A. Ducruix & R. Giegé, pp. 33–36. Oxford: IRL Press.
Lorber, B., Skouri, M., Munch, J.-P. & Giegé, R. (1993). *J. Cryst. Growth*, **128**, 1203–1214.
McPherson, A., Malkin, A. J., Kuznetsov, Yu. G. & Koszelak, S. (1996). *J. Cryst. Growth*, **168**, 74–92.
Miyashita, S., Komatsu, H. & Suzuki, Y. (1993). *Jpn J. Appl. Phys.* **32**, 1855–1857.
Miyashita, S., Komatsu, H., Suzuki, Y. & Nakada, T. (1994). *J. Cryst. Growth*, **141**, 419–424.
Muschol, M. & Rosenberger, F. (1995). *J. Chem. Phys.* **103**, 10424–10432.
Muschol, M. & Rosenberger, F. (1996). *J. Cryst. Growth*, **167**, 738–747.
Patton, W. F. (1995). *J. Chromatogr. A*, **698**, 55–87.
Riès-Kautt, M. & Ducruix, A. (1996). *Methods in Enzymology*, edited by C. Carter & R. Sweet, Vol. 276, pp. 23–59. San Diego: Academic Press.
Rosenberger, F. (1979). *Fundamentals of Crystal Growth, Vol. I: Macroscopic Equilibrium and Transport Concepts*, p. 406. Berlin: Springer.
Rosenberger, F., Vekilov, P. G., Muschol. M. & Thomas, B. R. (1996). *J. Cryst. Growth*, **167**, 1–27.
Sairam, M. R. (1991). *J. Endocrinol.* **130**, 415–424.

Skouri, M., Lorber, B., Giegé, R., Munch, J.-P. & Candau, J. S. (1995). *J. Cryst. Growth*, **152**, 209–220.
Sophianopoulos, A. J. & Van Holde, K. E. (1964). *J. Biol. Chem.* **239**, 2516–2524.
Steinrauf, L. K. (1959). *Acta Cryst.* **12**, 77–79.
Thomas, B. R., Vekilov, P. G. & Rosenberger, F. (1996). *Acta Cryst.* D**52**, 776–784.
Vekilov, P. G. & Rosenberger, F. (1996). *J. Cryst. Growth*, **158**, 540–551.
Vekilov, P. G., Monaco, L. A. & Rosenberger, F. (1995). *J. Cryst. Growth*, **156**, 267–278.
Vekilov, P. G., Monaco, L. A., Thomas, B. R., Stojanoff, V. & Rosenberger, F. (1996). *Acta Cryst.* D**52**, 785–798.
Wang, F., Hayter, J. & Wilson, L. J. (1996). *Acta Cryst.* D**52**, 901–908.
Wills, P. R., Nichol, L. W. & Siezen, R. J. (1980). *Biophys. Chem.* **11**, 71–82.
Wyatt, P. J. (1993). *Anal. Chim. Acta*, **272**, 1–40.